Local modification of elastic properties of polystyrene–polyethyleneoxide blend surfaces

H.-Y. Nie[a)]
Joint Research Center for Atom Technology, National Institute for Advanced Interdisciplinary Research, Higashi 1-1-4, Tsukuba, Ibaraki 305, Japan

M. Motomatsu[b)]
Joint Research Center for Atom Technology, Angstrom Technology Partnership, Higashi 1-1-4, Tsukuba, Ibaraki 305, Japan

W. Mizutani[c)] and H. Tokumoto[d)]
Joint Research Center for Atom Technology, National Institute for Advanced Interdisciplinary Research, Higashi 1-1-4, Tsukuba, Ibaraki 305, Japan

(Received 24 October 1994; accepted 13 March 1995)

Modifications of the phase-separated surface of polystyrene–polyethyleneoxide (PS-PEO) blend films were carried out by using an atomic force microscope. On PEO, contrary to PS, a scanning of a tip with large forces of 50 nN resulted in a modification of surface and increased the elastic stiffness. The modification was seen as regular stripes perpendicular to the scanning direction, which may be caused by the rearrangement of the PEO folding structure as a result of a balance of various forces during scanning. This rearrangement may increase the density of the films and hence causes the increase of the elastic stiffness. On the stripes, molecular images were obtained with friction force microscope, reflecting the folding structure of PEO. © *1995 American Vacuum Society.*

I. INTRODUCTION

Phase separation is an important issue in the research field of polymer composite. Recently, atomic force microscopy[1] (AFM) has been used to observe phase separations.[2–4] We have measured the surface topography of polystyrene–polyethyleneoxide (PS-PEO) blend films and found the phase separation of them,[4] where the PEO phase showed the spiral or layered structure.

In addition to the topographic feature, we can probe local elastic properties of materials through an interaction between the surface and tip.[5–11] The interaction can be measured by indenting the sample surface with the AFM tip.[7–9] In the course of the indentation, a force–distance curve is measured. The slope of the force–distance curve indicates how the sample surface is stiff against the applied force. Then we can deduce elastic properties, e.g., Young's modulus of sample surface by fitting the force curve to the Hertzian model[12,13] with an assumption of the tip apex geometry. There have been reports on mapping stiffness by modulating the sample height and recording the response of the cantilever,[14,15] which is called force modulation microscopy (FMM). We also used this technique in order to measure the elastic properties of the phase-separated PS-PEO blend films.

In this article, we concentrate on imaging elastic stiffness and modifying the film surface by varying forces between the tip and surface.

II. EXPERIMENT

We modified a commercial AFM system (SPA300, Seiko Instruments Inc.) that was equipped with a quadrant photodetector for detecting the deflection and torsion of the cantilever in order to obtain the topography and friction force microscope[16] (FFM) image, respectively. A rectangular shaped silicon nitride cantilever with a spring constant of 0.75 N/m and a resonance frequency of 88 kHz (Olympus Opt. Inc.) was used in this study. The cantilever was 0.8, 40, and 100 μm in thickness, width, and length, respectively. A single crystal silicon tip fabricated on an end of the cantilever was 2.8 μm in length and the radius of the tip apex was about 20 nm.

The deflection signal was used to measure force–distance curves when holding the tip at a particular location on the sample surface, or to image stiffness distribution during scanning. The torsional signal was also measured to check the ''cross-talk'' between the deflection and torsion of the cantilever during force–distance measurement. We found that the cross-talk in the present measurement system was as small as 2%–3%.

The oscillation of the sample height was realized by applying sinusoidal voltage to the vertical piezo scanner (PZT) on which the sample was fixed. The modulation frequency of 5 kHz was much higher than the cutoff frequency of the feedback loop of 0.5 kHz and lower than the resonance frequency of the piezo scanner (8 kHz) and the cutoff frequency of the photodetector system (1 MHz). The oscillation amplitude at a peak-to-peak value of about 1 nm did not degrade topographic images. The response of the cantilever to this oscillation was detected with a lock-in amplifier and was used to obtain images relevant to the stiffness of the sample surface.[14,15]

The solution of PS and PEO blended with 1:1 weight ratio in benzene was spin-coated onto a cleaved mica surface. Molecular weights for PS and PEO used as sources were 19 600 and 100 000, respectively. The thickness of the sample was

[a)]Electronic mail: hynie@nair.go.jp
[b)]Electronic mail: motomatu@jrcat.or.jp
[c)]Electronic mail: water@nair.go.jp
[d)]Electronic mail: htokumot@nair.go.jp

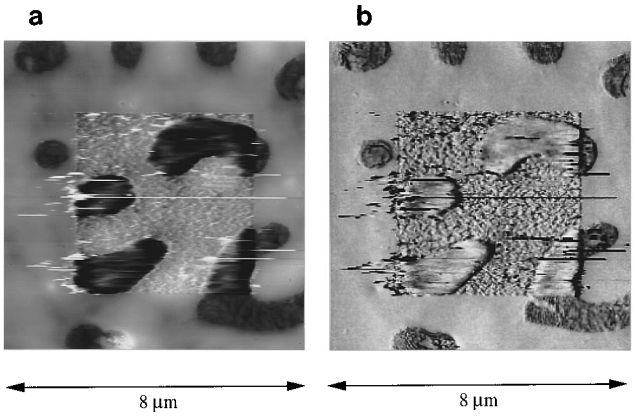

FIG. 1. Topography (a) and stiffness images (b) of phase-separated PS-PEO blend films, which were obtained simultaneously with small forces of 6 nN. The gray scale level of (a) is 0–167 nm and the darker areas represent depressed region corresponding to the PEO phase. The central area of 5 μm square corresponds to one experienced the large-force scanning of 50 nN.

about 200 nm. The sample was annealed at 90 °C for 24 h in moderate vacuum.

All measurements reported in this article were carried out in air with a humidity of about 60%. A scanning with large repulsive forces of 50 nN was done for examining the effect of forces on the sample surface. Images were obtained at constant repulsive forces of about 6 nN. The time constant of the lock-in amplifier was set to 1 ms. An image consisted of 256×256 pixel points. To acquire an image, we spent 8.5 min for both AFM and FMM images while 16 s for FFM images. Prior to the measurement, the deflection of the cantilever was calibrated by lifting up the sample by 10 nm and measuring the signal change of the photodetector. With a mica surface, the calibrated sensitivity was estimated to be about 30 mV/nm.

III. RESULTS AND DISCUSSION

A typical surface topography of the PS-PEO blend films is shown in Fig. 1(a). The average repulsive force during scanning was 6 nN. The central area of the image is the one that experienced a scanning with large forces of 50 nN, which is used for the discussion of the effect of forces on PS and PEO. We first consider the rest area that did not experience the large-force scanning. This part is the same as that already reported in Ref. 4 and exhibits the phase separation of PS and PEO. The depressed areas correspond to PEO, which exhibits the crystallized spiral or layered structure. Higher parts do not show the spiral or layered structure and therefore can be assigned as PS.

On the central area in Fig. 1(a), both PS and PEO surfaces are found to be scratched by the large-force scanning. However, the modified nature on PS and PEO is different. On PS, the corrugation amplitude is about 15 nm and the structure is locally rough and disordered, which may be caused by stirring molecular chains of PS with the tip. On PEO, the corrugation amplitude is 15–30 nm and the structure is round and smooth. This difference may be originated from the fact that PEO is crystallized but PS is not.

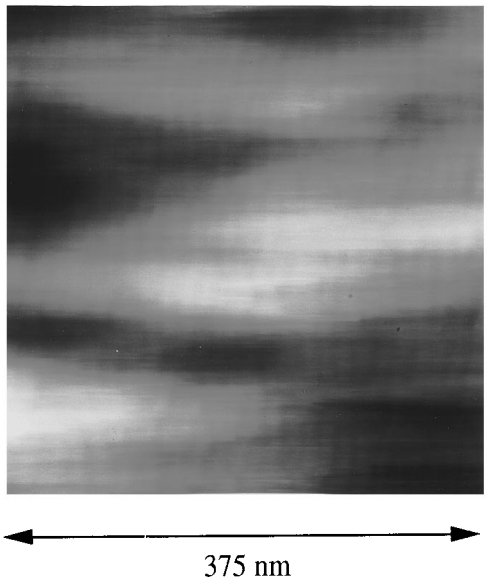

FIG. 2. Topography of PEO surface imaged with small forces of 6 nN after the large-force scanning of 50 nN. The gray scale level is 0–30 nm. There are stripes perpendicular to the large-force scanning direction.

Figure 1(b) shows the stiffness image simultaneously obtained with the topography in Fig. 1(a). Outside the central area, the response of the cantilever is found to be about 7% smaller on PEO than on PS, indicating PEO is softer than PS. In the central area, on the other hand, we can recognize the big change in the stiffness, as seen in Fig. 1(b). The response of the cantilever indicates that the PEO surface experiencing the large-force scanning becomes stiffer than the pristine one, and the difference in the response between that on PS and PEO becomes smaller down to 1%–2% there.

Figure 2 shows a typical topography of PEO surfaces that experienced the large-force scanning. This image was obtained with small forces of 6 nN. There are scratches along the scanning direction and overall surface features are round

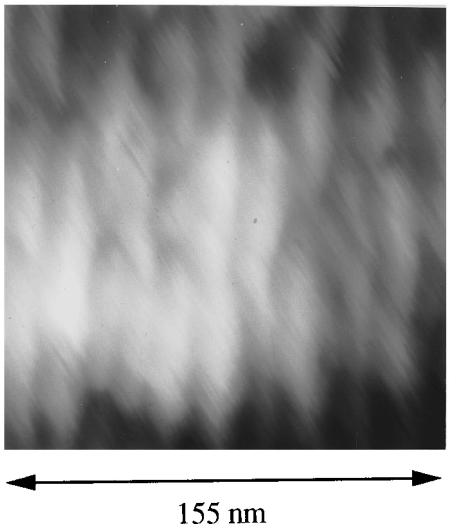

FIG. 3. Magnified topography, imaged with small forces of 6 nN, of the same PEO surface as shown in Fig. 2. The gray scale level is 0–20 nm. The stripes are clearly seen.

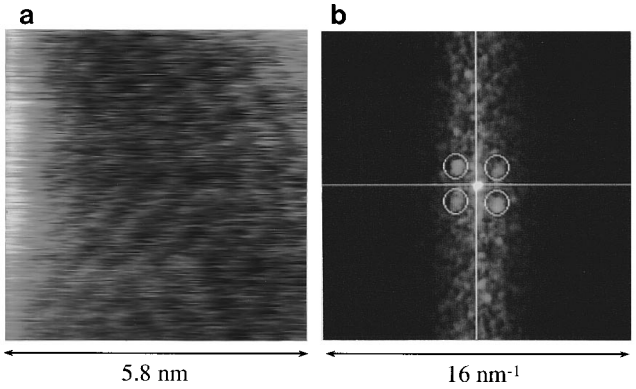

FIG. 4. (a) A friction force microscope (FFM) image obtained with small forces of 6 nN on the stripe region. (b) The Fourier spectrum of the raw data in the image. The four spots marked by circles in (b) indicate that there is a periodic structure in the FFM image with a period of about 0.6 nm.

and smooth. In addition to the scratches, regular stripes perpendicular to the scanning direction can be seen. Figure 3 is the magnified image of the stripes. The spacing between stripes is 15–20 nm and the corrugation height is 3–5 nm. The length of stripes is rather scattered with typical values of 50–100 nm. These stripes have never been observed on PEO surfaces without the large-force scanning. Therefore, the stripes can be induced by the large-force scanning. Similar stripe formation by the large-force scanning was also observed on a pure PEO sample. We consider that this stripe formation is closely related to the change in the stiffness image as will be discussed later.

On striped regions we obtained molecular resolution FFM images. A typical image is shown in Fig. 4(a), from which a faint periodic structure is visible without any filtering. The faintness of the periodic structure in the image was probably due to the fact that PEO is so soft that it may be easily deformed by the tip during scanning. Shown in Fig. 4(b) is the Fourier spectrum of the raw data in Fig. 4(a). The four spots indicated by circles in the spectrum show a periodicity corresponding to square arrays of the image. This structure was observed at various positions where the stripes were seen. There are periodic spots with a spacing of about 0.6 nm. It should be mentioned that, on the pristine PEO surface without the large-force scanning, a molecular resolution in FFM image was also obtained and the periodic feature was similar to that shown in Fig. 4. To explain this molecular image, we draw the crystal structure of PEO in Fig. 5(a), following a model based on x-ray analyses.[17] The long PEO chain folds many times, with a periodicity of 0.925 nm, at both the surface and bottom of the crystal layer as schematically illustrated in Fig. 5(b). The folding parts at the surface, depicted as filled circles in Fig. 5(a), form rectangular arrays with lattice distances of 0.656 and 0.652 nm. The molecular resolution shown in Fig. 4 may be attributed to these arrays, because of the good agreement with the measured distance of 0.6 nm in our FFM image.

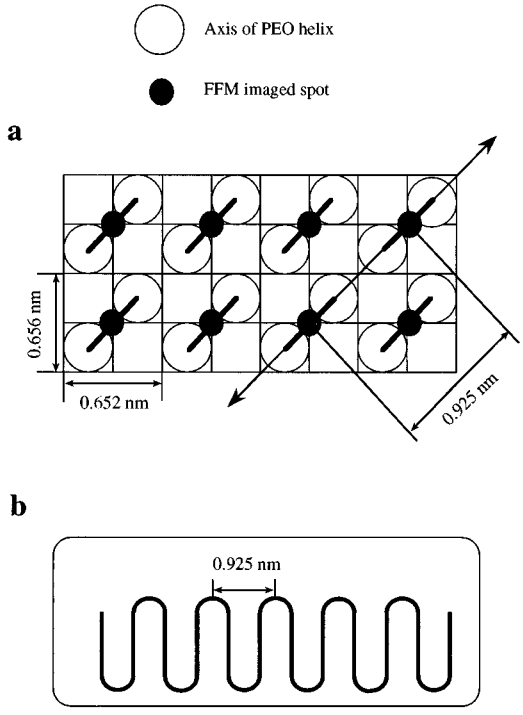

FIG. 5. A top view of PEO folding crystal structure (a) and its cut view along the line with arrows (b). Open circles denote axes of the PEO helices and filled circles correspond to folding parts of the chains at surfaces.

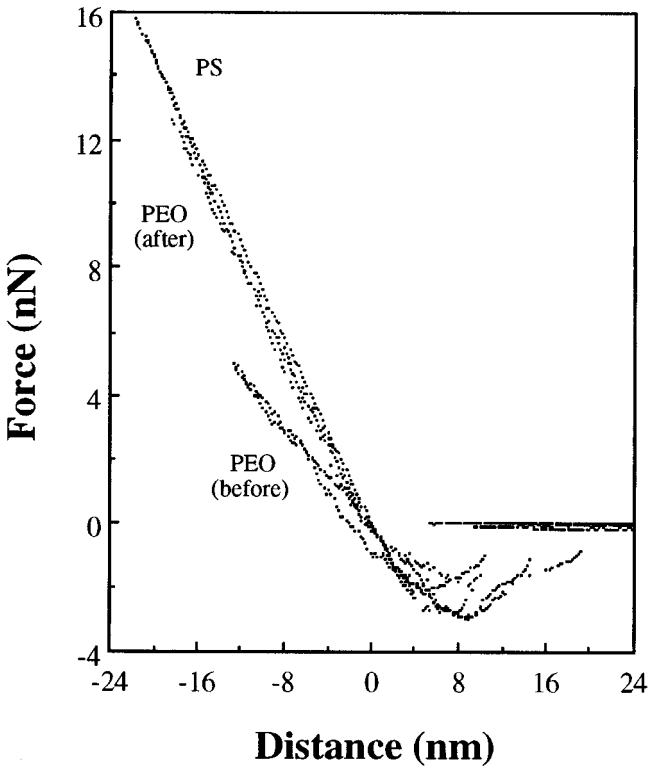

FIG. 6. Force-distance curves measured on PS and PEO surfaces. For PEO surfaces, two kinds of data for before and after the large-force scanning are shown. The speed of approaching and separating of the cantilever was 4 nm/s.

In order to deduce Young's modulus quantitatively, we measured force-distance curves on PS, PEO, and the large-force-scanned PEO areas. The results are shown in Fig. 6. The slopes for PEO changed clearly before and after the large-force scanning: the slope after the large-force scanning becomes steeper than that before the scanning and is close to

that of PS. By fitting the force curve to Hertzian model,[18] the Young's modulus of PS was deduced as 5.2 GPa. The Young's modulus of PEO was also deduced to be 0.2 and 5.0 GPa before and after the large-force scanning, respectively.

Here we shall discuss the formation mechanism of the observed regular stripes. During the large-force scanning, the tip pushes folding molecular chains down to some extent dependent on applied forces. There are also lateral forces accompanied by the scanning of the tip. This scanning process induces restoring forces (strains) in folding molecular chains, which force them back toward their initial positions. The balance of applied, lateral, and restoring forces determines the arrangement of folding molecular chains. From the model of the deformation of molecular chains, we can expect that there exists some difference in the folding periods between the pristine and large-force scanned PEO. However, it may be too small to be recognized by our FFM system.

The modification of the morphology is also considered to increase the density of molecular chains which in turn causes the increase of the Young's modulus from 0.2 to 5.0 GPa. From the topography shown in Fig. 1(a), the deformation of the PEO phases caused by the large-force scanning was estimated to be about 10 nm in average referring to their pristine parts. This deformation hence increases the density of the PEO molecular chains in a certain amount within the areas that experienced the large-force scanning. Unfortunately, we could not estimate the absolute value for the increase of the density because the thickness of the sample is 200 nm, which is too large to analyze the distribution of the deformation along the normal direction. By using PEO samples whose thickness is controlled, we plan to perform experiments to figure out the relationship between the increases of Young's modulus and the density of the molecular chains.

IV. CONCLUSIONS

The stiffness distribution of the phase-separated PS-PEO blend films was imaged by the force modulation microscopy. The elastic properties of PEO were modified after scanning with large forces of 50 nN. From force–distance curves, Young's moduli for PS, PEO, and the large-force-scanned PEO were deduced to be 5.2, 0.2, and 5.0 GPa, respectively. After the large-force scanning on PEO, there appeared regular stripes perpendicular to the scanning direction. A molecular resolution FFM image showing a periodicity of 0.6 nm was also obtained on stripes. In order to explain modifications of elastic properties and morphology on PEO surfaces induced by the large-force scanning, we proposed the following model: the density of molecular chains increases as a result of the balance of applied, lateral, and restoring forces during the scanning.

ACKNOWLEDGMENTS

The authors thank T. Shimizu, T. Inoue, and H. Yokoyama for their assistance and discussion in the initial stage of this work. The authors are grateful to Y. Nakagawa of Toray Research Center for discussion on PEO materials. One of the authors (H.Y.N.) acknowledges a fellowship supported by the Research Development Corporation of Japan (JRDC). This work was supported in part by the New Energy and Industrial Technology Development Organization (NEDO).

[1]G. Binnig, C. F. Quate, and Ch. Gerber, Phys. Rev. Lett. **56**, 930 (1986).
[2]M. Maaloum, D. Ausserre, D. Chatenay, and Y. Gallot, Phys. Rev. Lett. **70**, 2577 (1993).
[3]M. Motomatsu, H.-Y. Nie, W. Mizutani, and H. Tokumoto, Jpn. J. Appl. Phys. **33**, 3775 (1994).
[4]M. Motomatsu, W. Mizutani, H.-Y. Nie, and H. Tokumoto, in *Proceedings of Forces in Scanning Probe Microscopies*, edited by H.-J. Güntherodt, ASI E286 (Kluwer Academic, Dordrecht, 1995), p. 331.
[5]D. Tománek, G. Overney, H. Miyazaki, S. D. Mahanti, and H.-J. Güntherodt, Phys. Rev. Lett. **63**, 876 (1989).
[6]S. P. Jarvis, A. Oral, T. P. Weihs, and J. B. Pethica, Rev. Sci. Instrum. **64**, 3515 (1993).
[7]D. M. Schaefer, A. Patil, R. P. Andres, and R. Reifenberger, Appl. Phys. Lett. **63**, 1492 (1993).
[8]A. L. Weisenhorn, M. Khorsandi, S. Kasas, V. Gotzos, and H.-J. Butt, Nanotechnology **4**, 106 (1993).
[9]P. Tangyunyong, R. C. Thomas, J. E. Houston, T. A. Michalske, R. M. Crooks, and A. J. Howard, Phys. Rev. Lett. **71**, 3319 (1993).
[10]D. Anselmetti, Ch. Gerber, B. Michel, H.-J. Güntherodt, and H. Rohrer, Rev. Sci. Instrum. **63**, 3003 (1992).
[11]N. A. Burnham, R. J. Colton, and H. M. Pollock, Nanotechnology **4**, 64 (1993).
[12]L. D. Landau and E. M. Lifshitz, *Theory of Elasticity* (Pergamon, New York, 1959), p. 30.
[13]K. L. Johnson, *Contact Mechanics* (Cambridge University Press, Cambridge, 1985), p. 84.
[14]P. Maivald, H.-J. Butt, S. A. C. Gould, C. B. Prater, B. Drake, J. A. Gurley, V. B. Elings, and P. K. Hansma, Nanotechnology **2**, 130 (1991).
[15]M. Radmacher, R. W. Tillmann, M. Fritz, and H. E. Gaub, Science **257**, 1900 (1992).
[16]G. Meyer and N. M. Amer, Appl. Phys. Lett. **57**, 2089 (1990).
[17]Y. Takahashi and H. Tadokoro, Macromolecules **6**, 672 (1973).
[18]The deduced Young's modulus has a weak dependence upon Poisson's ratio. In our case we assumed that Poisson's ratio was 0.33, following the literature of L. E. Nielsen, *Mechanical Properties of Polymers* (Reinhold, New York, 1967), p. 7.